Available online at www.sciencedirect.com
SCIENCE DIRECT®
Journal of Virological Methods 115 (2004) 19–30
Journal of Virological Methods
www.elsevier.com/locate/jviromet

A simple mathematical formula for stoichiometry quantification of viral and nanobiological assemblage using slopes of log/log plot curves

Dan Shu, Lisa Huang, Peixuan Guo*

Department of Pathobiology and Purdue Cancer Research Center, B-36 Hansen Life Science Research Building, Purdue University, West Lafayette, IN 47907, USA

Received 15 May 2003; received in revised form 18 August 2003; accepted 20 August 2003

Abstract

In nanotechnology, biomolecular assemblies serve not only as model systems for the construction of nanodevices, but they can also be used directly as templates for the formation of nanostructures. Biological nano-building blocks can either be isolated as complete functional units from living cells or viruses (biological "Top down" approach) or formed by biomolecular assembly from recombinant or synthetic components ("Bottom up" approach). In both cases, rational design of nanostructures requires knowledge of the stoichiometry of the biological structures, which frequently occur as multimers, i.e., the morphological complex is composed of multiple copies of one or more macromolecules. In this paper, a method is described for the stoichiometric quantification of molecules in bio-nanostructures. The method is based on using dilution factors and relative concentrations rather than absolute quantities, which are often difficult to determine, especially in short-lived assembly intermediates. The approach exploits the fact that the larger the stoichiometry of the component is, the more dramatic is the influence of the dilution factor (decrease in concentration) on the reaction. We established and used the method to determine the stoichiometry of components of bacterial virus phi29. The log of dilution factors was plotted against the log of reaction yield. The stoichiometry Z was determined with the equation $Z = -1.58 + 2.4193T - 0.001746T^2$ [$T \in (0,1000)$, or $\angle\alpha \in (0^\circ, 89.9^\circ)$], where T is the slope of the curve (tangent of $\angle\alpha$, which is the angle between the x-axis and the concentration dependent curve). Z can also be determined from a standard table given in this report. With the bacteriophage phi29 in vitro assembly system, up to 5×10^8 infectious virions per ml can be assembled from 11 purified components, giving our method a sensitivity of nine orders of magnitude. We confirmed the stoichiometries of phi29 components that were determined previously with microscopic approaches. The described method also responded to programmed stoichiometry changes, which were generated by assembling the phi29 DNA packaging motor from modified pRNA (DNA-packaging RNA) molecules forming a trimer of dimers or a dimer of trimers, instead of the wild-type hexamer.

Keywords: Nanotechnology; Biomolecular assembly; Stoichiometric quantification

1. Introduction

Viral components hold great potential for nanotechnology because viruses, due to their genome size and life cycle restrictions, typically have to assemble functional structures efficiently from a limited number of components, following a comparatively simple construction plan (Bazinet and King, 1985; Black, 1989; D'Halluin et al., 1978; Guo, 1994). Consequently, viral structures are typically formed by multimers of gene products. In order to apply such viral structures in nanotechnology, knowledge of the stoichiometry of biological components is essential. However, direct quantitation in many cases is not straightforward, because the biological material in nanoscale is often too soft and too small for atomic force microscopy, does not give high enough resolution in negatively stained preparations, and does not provide enough contrast in (cryo) electron microscopy due to the low electron density, especially for nucleic acids.

Approaches in nanotechnology are often distinguished between "Top down" and "Bottom up" approaches (Balzani et al., 2002; Niemeyer, 2002; Seeman and Belcher, 2002). However, in virology, functional nanostructures have been studied both by "Bottom up" and "Top down" approaches for decades (Earnshaw and Casjens, 1980; Kaiser et al., 1975; Kerr and Sadowski, 1974; Murialdo and Becker, 1977; Pruss et al., 1975). The "Top down" approaches include structural

* Corresponding author. Tel.: +1-765-494-7561; fax: +1-765-496-1795.
E-mail address: guop@purdue.edu (P. Guo).

0166-0934/$ – see front matter © 2003 Published by Elsevier B.V.
doi:10.1016/j.jviromet.2003.08.015

studies on viral components or the dissection of the complete viral particles into subunits or single molecules, using various methods of molecular biology (Bancroft et al., 1967; Edvardsson et al., 1976; Hsiao and Black, 1977; King and Casjens, 1974; Leibowitz and Horwitz, 1975; Murialdo and Becker, 1977). The bottom up approaches exploit the efficiency of viral assembly. Not only viral components, but also complete infectious virions can be assembled in vitro from single molecules or synthetic materials (Becker et al., 1977; Guo et al., 1986; Hohn, 1975; Israel et al., 1967; Kaiser and Masuda, 1973; Kerr and Sadowski, 1974; Lee and Guo, 1995a; Miyazaki et al., 1978; Pruss et al., 1975; Skehel and Joklik, 1969; Wilhelm and Ginsberg, 1972). The completely defined in vitro assembly of RNA viruses was first demonstrated with tobacco mosaic virus (Fraenkel-Conrat and Williams, 1955). For DNA viruses, in vitro assembly with the exclusive use of purified recombinant proteins and synthetic nucleic acid was first demonstrated for bacteriophage phi29 (Lee and Guo, 1995a). The contributions of virology to nanotechnology include the use of complete virions as well as the modification of self-assembling viral components (Carbone and Seeman, 2002; Dujardin et al., 2003; Hyman et al., 2002; Lee et al., 2002; Moll et al., 2002; Shu and Guo, 2003). Both in "Top down" and "Bottom up" approaches, a stoichiometry determination of the components in the nanostructure is critical. This study aims to derive a simple technique for the quantification of nano-assemblages, using bacterial virus phi29 as a model.

Many biological processes involving complex systems utilize multiple components in multi-step reactions. Quantitative analysis of these systems has been complicated due to the shortage of plausible methods to study them. For instance, in rapid reactions, it is very difficult to isolate and characterize the intermediates or to elucidate intermediate states of the reaction, especially in complex biological systems.

A variety of biological systems and molecular processes have been analyzed by mathematical methods (Becker et al., 1977; Cohen et al., 1986; Israel et al., 1967; Thomas and Prevelige, 1991; Waterman et al., 1987; White et al., 1988). One method used widely to analyze binding equilibrium in ligand–receptor interaction is the application of the Hill equation, which was originally applied by A.V. Hill in 1910 to determine the binding of oxygen to hemoglobin (Hill, 1910). This equation provides a method not only to measure the affinity of a ligand for a receptor, but also to estimate the number of ligand molecules that are needed for receptor binding in order to execute appropriate functions. The number of ligands can only be estimated by the Hill coefficient under conditions where extreme positive cooperativeness occurs. That is, the binding of the second molecule is dependent on the first one. For this reason, the Hill coefficient is only an indication of the interaction coefficient reflecting cooperativeness rather than a reliable method for stoichiometry determination (Monod et al., 1965). In addition, in a simple sequential or an independent binding reaction with up to ten binding sites for neutral cooperativeness, the Hill coefficient is always less than two (Weiss, 1997). To this end, it would be desirable to have a more reliable and simple method to determine the stoichiometry of structural components or enzymes that actively participate in intermediate reactions.

Recently, binomial distribution has been used to determine the stoichiometry of the components in phi29 assembly (Chen et al., 1997; Lee and Guo, 1994, 1995a; Trottier and Guo, 1997). Determination of the RNA stoichiometry by aforementioned methods has led to the discovery of a novel mechanism in viral DNA packaging (Guo et al., 1998; Hendrix, 1998; Zhang et al., 1998). It has been found that six packaging RNAs (pRNA) interact hand-in-hand via two loops to form a hexagonal complex to gear the DNA translocation machine, thus predicting that viral genomic DNA packaging (encapsidation) is accomplished by a mechanism similar to the driving of a bolt by a hex nut (Chen and Guo, 1997b; Guo et al., 1998; Hendrix, 1998; Zhang et al., 1998).

The stoichiometry study takes advantage of a highly sensitive in vitro phage phi29 assembly and assay system recently developed in this lab (Lee and Guo, 1994,1995a,b). With this system, 10^8 infectious virions per milliliter can be assembled from eleven purified components in vitro without any background. Eliminating only one of the 11 components results in no plaque formation. The assembly process can be summarized into the following steps in vitro (Fig. 1)—the isolation of pre-formed procapsids, the binding of six pRNAs to each procapsid, the packaging of genomic DNA with the aid of pRNAs and gp16 fueled by ATP hydrolysis, and the addition of the tail protein gp9 followed by lower collar protein gp11 and anti-receptor gp12. Up to 90% of the added phi29 DNA can be packaged into the pre-formed procapsids

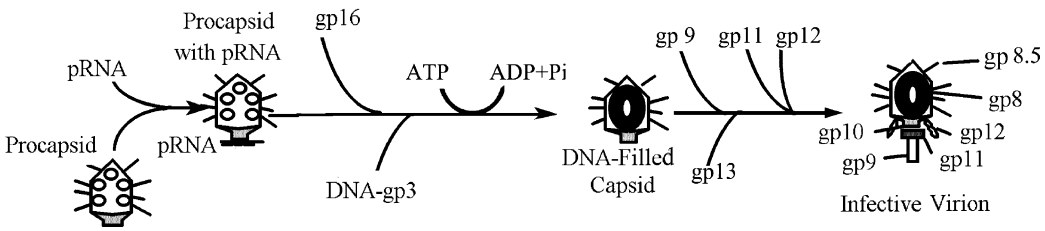

Fig. 1. Assembly pathway of bacterial virus phi29 in vitro.

composed of 180 copies of scaffolding protein gp7 (Guo et al., 1991), 235 copies of capsid protein gp8 and 12 copies of connector protein gp10 (Guasch et al., 2002; Simpson et al., 2000). The DNA-filled procapsids can be converted into infectious virions up to 10^8 per milliliter in vitro, with the addition of the nine copies of tail protein gp9, twelve copies of lower collar protein gp11, and twelve copies of appendage anti-receptor, which is composed of two subunits of gp12. Replacing any one of active components with an inactive component results in zero plaque formations. With an eighth-order sensitivity, this system provides a convenient assay for the deduction of a formula for stoichiometry determination.

Now that the pilot experiments have documented the feasibility of using this approach to determine the stoichiometry of phi29 components, it is time to address the general application and to deduce a general formula and table of standard curves for the application of other biological systems. The in vitro phi29 assembly system involves 11 components, including protein or protein oligomers, enzymes, RNA, genomic DNA and ATP. The copy number for each of the 11 components required for the assembly of one virion varies from one (the genome or procapsid) to 9000 (ATP). The stoichiometry of most structural components, including genomic DNA, procapsid, pRNA, gp9, gp11 and gp12 (Guo et al., 1987,1998) in assembly has been explicitly determined (Peterson et al., 2001; Trottier and Guo, 1997). These components serve as standard controls for establishing the constants in the formula deduced.

2. Experimental procedures

2.1. Synthesis of pRNAs

RNAs were prepared as described previously (Zhang et al., 1994). Briefly, DNA oligos were synthesized with the desired sequences and used to produce double-stranded DNA by PCR. The DNA products containing the T7 promoter were cloned into plasmids. RNA was synthesized with T7 RNA polymerase by run-off transcription and purified from a polyacrylamide gel. All mutant RNAs made by in vitro transcription were purified by excision from 8 M urea denaturing gels and quantified by both comparison with standard RNA in gels and UV absorbance with one OD_{260} equal to 40 μg/ml of pRNA. The sequences of both plasmids and PCR products were confirmed by DNA sequencing.

2.2. Preparation of other components needed for the assembly of the infectious phi29 virion in vitro

The purification of procapsids, the DNA-packaging protein gp16, DNA–gp3 (Guo et al., 1986), the preparation of the tail protein gp9, lower collar proteins gp11, anti-receptor gp12, and morphogenetic factor gp13 (Lee and Guo, 1995a) have been described previously.

2.3. Isolation of RNA dimers and trimers from native polyacrylamide gels

Eight percent native polyacrylamide gels (Chen and Guo, 1997a) were prepared in TBM buffer (89 mM Tris, 200 mM boric acid, 5 mM $MgCl_2$, pH 7.6). About 0.5 μg of total pRNA in TBM was loaded in each lane. Equal amounts of each of the two types (for example, pRNA A-I′ and I-a′) or three (for example, A-b′, B-c′ and C-a′), respectively, of pRNA were used for the production and purification of pRNA dimers and trimers. Tritiated pRNA A-b′ was incorporated into dimers or trimers and subjected to electrophoresis in 8% native PAGE made in TBM. The pRNA dimer and trimer bands were excised from the gels and eluted using elution buffer (0.5 M NH_4OAC, 0.1 mM EDTA, 0.1% SDS, 5 mM $MgCl_2$) at 37 °C overnight. The eluted complexes were then kept in TBM buffer at 4 °C for further use or frozen at −20 °C.

2.4. Separation of pRNA complexes by sucrose gradient sedimentation

Linear 5–20% sucrose gradients were prepared in TBM buffer. The pRNA mixtures containing multimers were loaded onto the top of the gradient. To separate dimers from trimers, samples were spun at 45,000 rpm for 13 h at 4 °C in a SW55 rotor. To separate dimers from monomers, samples were spun at 50,000 rpm for 14.5 h at 4 °C in a SW55 rotor. After sedimentation, fractions were collected at 15 drops each and subjected to scintillation counting (Chen et al., 2000).

2.5. In vitro production of the infectious phi29 virion

In vitro assembly was undertaken with decreasing concentrations, via a two-fold serial dilution of the component to be tested. In each dilution study, only the component to be tested was changed and kept limited while all other assembly components were in excess. The procedures for the assembly of the infectious phi29 virion in vitro (Lee and Guo, 1995a) have been described previously. Briefly, 1 μl pRNA in RNase free H_2O was mixed with 10 μl of purified procapsids (0.4 mg/ml) and then dialyzed on a 0.025 μm type VS filter membrane (Millipore) against 1 × TBE (2 mM EDTA, 89 mM Tris borate, pH 8.0) for 15 min at room temperature. The mixture was subsequently transferred for another dialysis against TMS (100 mM NaCl, 10 mM $MgCl_2$, 50 mM tris/pH 7.8) for an additional 30 min. The pRNA-enriched procapsids were then mixed with gp16, DNA–gp3, and ATP (1.4 mM final concentration) to complete the DNA packaging reaction. After 30 min room temperature incubation, gp9, gp11, gp12, and gp13 were added to the DNA packaging reactions to complete the assembly of

Table 1
Experimental data for stoichiometry and slopes

Components for phi29 virion assembly	Function	Total subunits/ virion	Stoichiometry	∠ of curve (degrees)	Slopes (tan) empirical	Slopes (tan) theoretical
DNA-gp3	Genome complex	1	1	45 ± 4	1	1
Procapsid	Hold DNA	1	1	47 ± 3	1.07	1
pRNA trimer	DNA-packaging	6	2	56 ± 2	1.48	1.48
pRNA dimer	DNA-packaging	6	3	64 ± 5	2.05	2.05
pRNA monomer	DNA-packaging	6	6	72 ± 3	3.08	3.14
Gp9	Tail knob protein	10	9	77 ± 2	4.33	4.33
Gp11	Lower collar	12	12	79 ± 1	5.14	5.67
Gp12	Anti-receptor	24	12	80 ± 2	5.67	5.67

infectious virions, which were assayed by standard plaque formation.

2.6. Deduction of a formula for stoichiometry determination

Each component of the phi29 in vitro viral assembly system was assayed by serial dilution while keeping all other components optimal or in excess. The relative concentration (*x*-axis, from low to high) was plotted against the yield (*y*-axis) of phi29 virions assembled (PFU/ml). The log scale was used for both the concentration and the yield, with the unit length of the log scale of *x*-axis equal to that of *y*-axis (Chen et al., 1997; Guo, 2002a; Trottier and Guo, 1997). The angle between the *x*-axis and the concentration dependent curve was measured. A value of tangent (slope tan) for the angle was determined. Slopes of such connection dependent curves for procapsid, DNA–gp3, pRNA trimer, dimer, and monomer, as well as gp9, gp11, and gp12 were obtained (Table 1). The slopes (tan) of all curves were plotted against their stoichiometry. A computer program, Cricket Graph, was used to find a best-fit curve and to deduce the formula for stoichiometry determination.

3. Results

The nomenclature of pRNA used in previous publications will be used in this report. To simplify the description of these mutants, uppercase and lowercase letters are used to represent the right and left-hand loop sequences of the pRNA, respectively (Fig. 3). The same letter in upper and lower cases symbolizes a pair of complementary sequences. For example, in pRNA A-a′, the right loop A ($5'GGAC_{48}$) and the left loop a′ ($3'CCUG_{82}$) are complementary, while in pRNA A-b′, the four bases of the right loop A are not complementary to the sequence of the left loop b′ ($3'UGCG_{82}$).

3.1. Stoichiometry of phi29 in in vitro assembly system

The highly sensitive in vitro phi29 assembly system has been used to determine stoichiometry of components needed for phi29 assembly (Table 1) (Chen et al., 1997; Lee and Guo, 1994,1995a; Trottier and Guo, 1997). The log/log plot method only deals with the functional unit (oligo or complex), not the copy number of the subunits, as described herein. The procapsid, despite containing the 180 copies of scaffolding protein gp7, the 235 copies of capsid protein gp8, and 12 copies of the portal protein gp10, is a complex that is regarded as one component. The DNA–gp3 is also considered as one component since the DNA and terminal protein gp3 are covalently linked. The log/log plot has revealed that the slope of the log/log concentration dependent curve for procapsid is one; therefore, one copy of procapsid is needed for the assembly of one virion (Chen et al., 1997; Lee and Guo, 1994,1995a; Trottier and Guo, 1997). The genomic DNA–gp3 acts in the same way. The stoichiometry for gp11 and gp12 have been determined to be six, 12 and 12, respectively, using the methods of log/log Slope Assay (Chen et al., 1997), binomial distribution (Chen et al., 1997; Trottier and Guo, 1997), common multiples of two and three (Guo et al., 1998; Guo, 2002b), migration rates in gel (Peterson et al., 2001), and EM (Anderson et al., 1966).

In 1998, two labs independently demonstrated that pRNA forms *hexamers* as part of the phi29 motor (Guo et al., 1998; Zhang et al., 1998) (see also minireview in *Cell* (Hendrix, 1998)). Later, Carrascosa's group noticed a pRNA hexamer by cryo-EM (Ibarra et al., 2000). In contrast, the same cryo-EM approach by Michael Rossmann and coworkers reported a pRNA pentamer (Morais et al., 2001; Simpson et al., 2000). One explanation by the latter group was that pRNA hexamers are formed initially, but after binding, one of the pRNAs dissociates from the procapsids, leaving five pRNAs still bound. The contradictory results by these two groups with similar cryo-EM approach is possibly due to the difficulty in resolving EM image because of the low electron density of RNA, as well as the interference of the five-fold symmetrical procapsid shell around the pRNA complex. The pentamer speculation is also contrary to the finding by genetics and biochemical approaches. These approaches revealed that (1) the stoichiometry of pRNA is the least common multiple of two and three (Guo et al., 1998), that is, six; (2) a clear demonstration that pRNA binds to the dodacamer connector, not the procapsid (Garver and Guo, 1997)

as proposed by Rossmann's group; (3) dimers are the binding unit and the building blocks of hexamers (Chen et al., 2000; Guo et al., 1998; Zhang et al., 1998); (4) mixing six different inactive pRNA monomers that have been engineered to form a hexameric ring generates a high level of activity (Guo et al., 1998). As demonstrated here, purified pRNA trimers have the highest specific activity (Fig. 5). It was found that the explanation by the latter group, that formation of petamer is a result of dissociation of one pRNA subunit from the hexamer could not be sustained by the data revealing that covalently linked pRNA dimers are active in DNA packaging (Chen et al., 2000).

Although it has been found that six pRNAs form a hexamer as a vital part of the DNA translocating motor (Fig. 3), the hexamer can be assembled in vitro from individual pRNA molecules, or complexes (Fig. 4) (Guo et al., 1998; Hoeprich and Guo, 2002; Zhang et al., 1998). If the hexamer is assembled from one A-a′ or B-b′ monomer or six monomer A-b′, B-c′. C-d′, D-e′, E-f′, F-a′ (Fig. 4A) (Guo et al., 1998), the monomer is regarded as one component and the stoichiometry of pRNA monomer is six (Chen et al., 1999). If the hexamer is assembled from purified dimer composed of (I-a′)/(A-i′) (Figs. 2 and 4B), the dimer is regarded as one component, and the stoichiometry for dimer RNA is three (Chen et al., 2000; Guo et al., 1998). If the hexamer is assembled from purified (A-b′)/(B-c′)/(C-a′) trimer (Fig. 4C), the trimer is regarded as one component and the stoichiometry

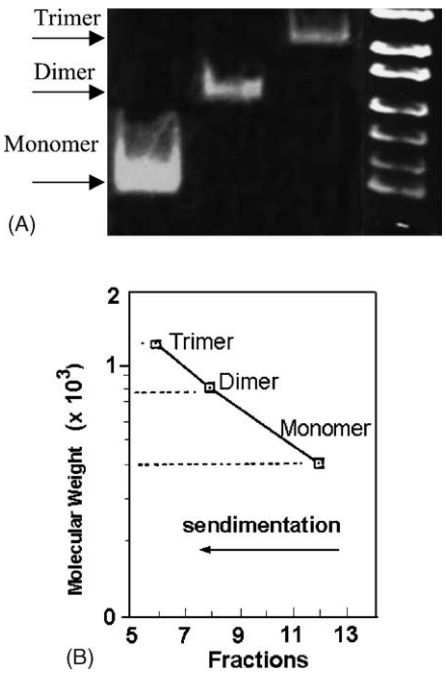

Fig. 2. Purification and identification of monomer, dimer and trimer of pRNA. (A) By native polyacrylyminde gel. (B) Elucidation of correlation between the molecular weight of the oligomers and the migration distance in sucrose gradient to confirm the size of pRNA in panels A and B. A smooth line is observed, which agrees with the typical distance versus log molecular weight plot.

for trimer-RNA is two (Chen et al., 1999; Guo et al., 1998). It was found that gp12 formed a dimer before being packaged into a phi29 assembly intermediate (Villanueva et al., 1981; Villanueva and Salas, 1981), and each dimeric gp12 is regarded as one component. Therefore, the stoichiometry of gp12 is 12, instead of 24, disregarding the fact that there are 24 copies of gp12 in each phi29 virion. Purified tail protein gp9, expressed in *Escherichia coli*, has been shown to be active in in vitro phi29 assembly. The absolute copy number of gp9 in one virion has been reported to be nine (Peterson et al., 2001).

3.2. Determination of slopes of log/log plot curves for concentration versus yield

The basis for the design of this method is that the slope of the curve in the log/log plot of the concentration versus the product for each component is the intrinsic parameter reflecting the stoichiometry of the component, since the larger the stoichiometry of the component, the more dramatic the influence of the component concentration (dilution factor) on the reaction. In the plot curve, *y*-axis is the log of the yield of the reaction, and *x*-axis is the log of the step-up concentration, or the log of the inverse of the dilution factor starting with high dilution. The larger the stoichiometry of one component is, the larger the slope of the log/log-plot-curve for this component will be. The slope is defined as the tangent of the angle between the curve and the *x*-axis. When plotting the curve for measuring the slope, the unit length for the *x*-axis (log of concentration) must be the same as that in the *y*-axis (log of yield).

In vitro assembly was performed with decreasing concentrations via two-fold serial dilution of the component to be tested. In each dilution study, only the component to be tested was changed and kept limited while all other assembly components were in excess. We have shown that all of these components, including procapsid, DNA–gp3, pRNA, gp16, gp9, gp11, gp12, and gp13 can be used to assemble infectious virions in vitro without involvement of the phi29 host cell (Lee and Guo, 1995a). The log of the yield, measured as plaque-forming unit per milliliter (PFU/ml), was plotted against the log of the concentration of each component.

3.3. Descending of trimeric, dimeric and monomeric pRNA slopes of log/log plot curves

There are two loops, the left and right hand loops (Chen et al., 1999), in the predicted secondary structure of the pRNA (Fig. 3). Sequences of these two loops (bases 45–48 of right hand loop and bases 85–82 of left-hand loop) are complementary. However, extensive studies (Chen et al., 1997, 1999, 2000; Garver and Guo, 2000; Trottier et al., 2000; Chen and Guo, 1997a,b; Zhang et al., 1998) have revealed that these two sequences interact intermolecularly, allowing the formation of pRNA oligomers. Several pRNAs with mutated left and right hand loop sequences were constructed.

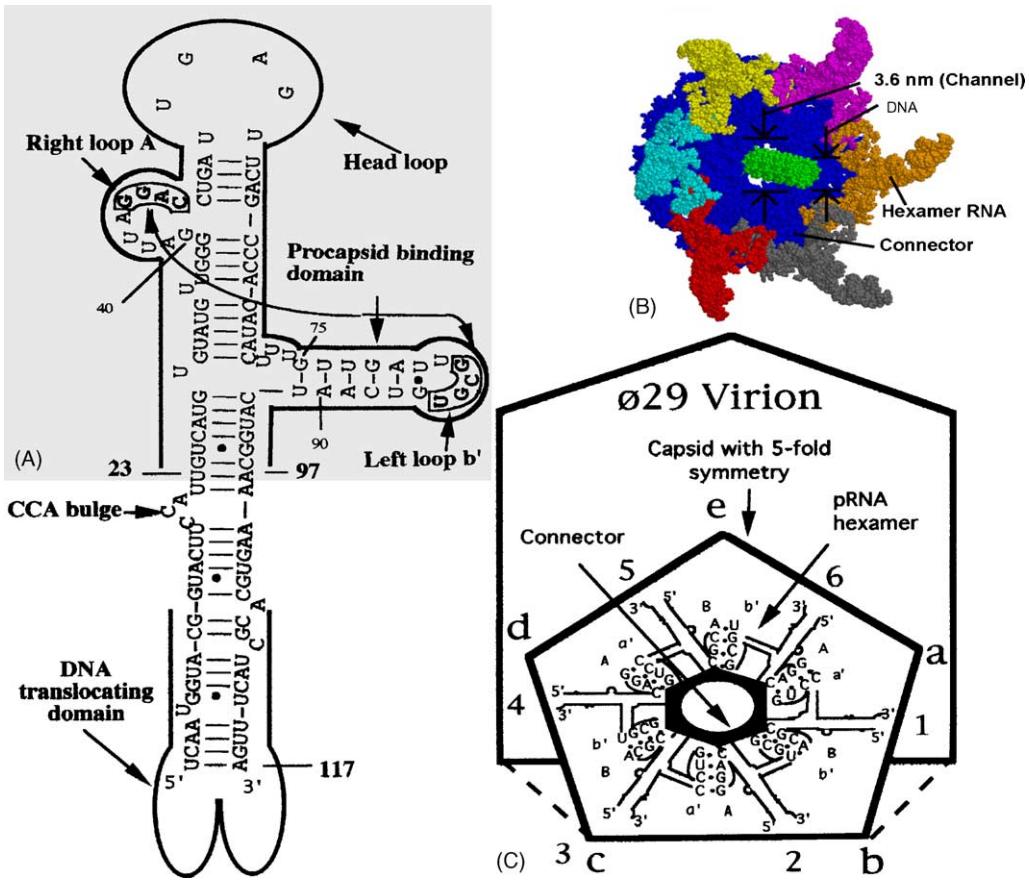

Fig. 3. Secondary structure of pRNA on phi29 bacteriophage. (A) Secondary structure of wild-type pRNA A-b′. The binding domain (shaded area) and the DNA translocation domain are marked with bold lines. The four bases in the right and left loops, which are responsible for inter-RNA interactions, are boxed. (B) A 3D model of the viral packaging motor. (C) Diagrams depicting the formation of pRNA hexamer ring and its location in the phi29 DNA packaging machine. Hexamer formation is via right-and-left-loop sequence interactions of pRNA A-b′ and B-a′ (Hoeprich and Guo, 2002).

3.3.1. Stoichiometry of pRNA monomer; a set of six inter-locking pRNAs (Guo et al., 1998)

DNA packaging activity is achieved by mixing six mutant pRNA monomers A-b′, B-c′. C-d′, D-e′, E-f′, and F-a′ (Fig. 4A). Six monomers will form a hexamer, thus the stoichiometry for a monomer is six. The angle between the *x*-axis and RNA monomer dilution curve is 72°±3° (Table 1, Fig. 5).

3.3.2. Stoichiometry of pRNA dimer; a set of two interlocking pRNAs (Guo et al., 1998)

Mixing of two mutant pRNAs with trans-complementary loops restored DNA packaging activity. For example, pRNAs I-a′ and A-I′ were inactive in DNA packaging alone, but when mixed together restored DNA packaging activity (Fig. 4B). This result can be explained by the trans-complementarily of pRNA loops, i.e. the right hand loop I of pRNA I-a′ could pair with the left hand loop i′ of pRNA A-i′. Since mixing two inactive pRNAs with interlocking loops, such as when pRNA I-a′ and A-i′ are mixed in a 1:1 molar ratio, resulted in production of infectious virions, the stoichiometry of the pRNA is predicted to be a multiple of two (Fig. 4). When I-a′ and a′-I were mixed, a dimer was produced and purified from gel (Fig. 2A). Three dimers will form a hexamer, thus, the stoichiometry for a dimer is three. The angle between the *x*-axis and RNA dimer dilution curve is 64° ± 5° (Table 1, Fig. 5).

3.3.3. Stoichiometry of pRNA trimer; a set of three interlocking pRNAs (Guo et al., 1998)

Three pRNAs, A-b′, b-c′, and C-a′, can form a trimer (Figs. 2 and 4C). When tested alone, each individual pRNA shows little or no activity (Fig. 4). When any two of the three mutants are mixed, again little or no activity is detected. However, when all three pRNAs are mixed in a 1:1:1 ratio, DNA packaging activity is fully restored. The lack of activity of two mutant pRNAs in mixture and the restoration of activity with mixing of three mutant pRNAs are expected since the mutations in each RNA are engineered in such a way that only the presence of all three RNAs will produce a closed ring. The fact that the three inactive pRNAs are fully active when mixed together suggests that the number of pRNAs in the DNA packaging complex is a multiple of three. When A-b′, B-c′, and C-a′ were mixed, pRNA trimers

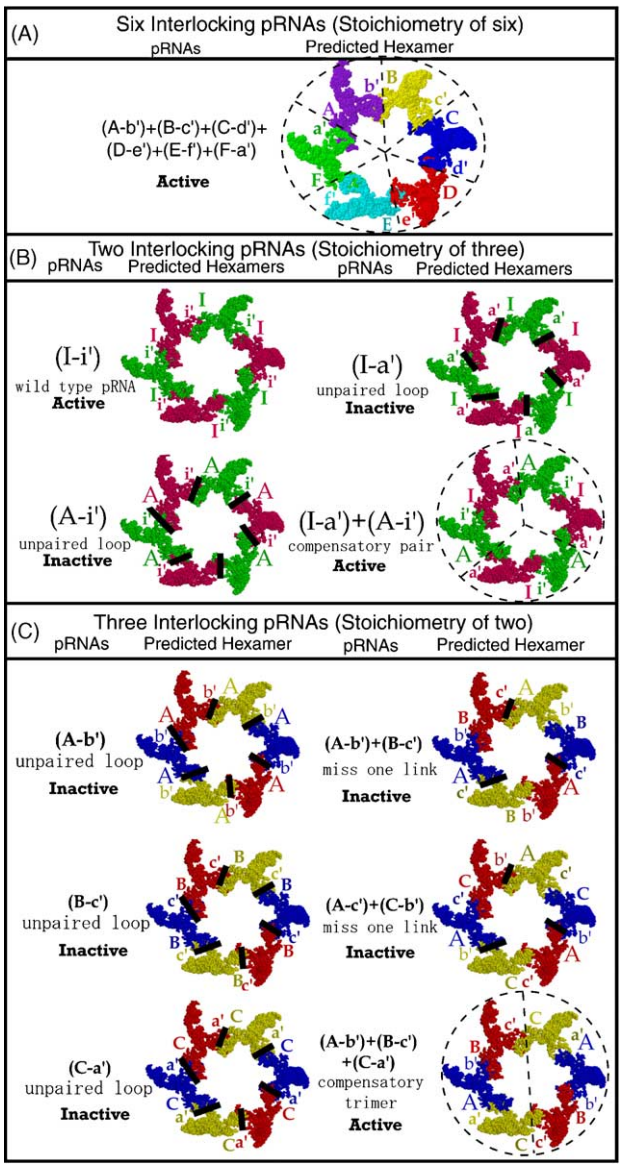

Fig. 4. Interlocking pRNAs of loop-loop interaction in monomer (A), dimer (B) and trimer (C). I-i′ in B represents the wild type pRNA loops.

were produced (Fig. 2). Two purified trimers will form a hexamer, thus the stoichiometry for a trimer is two. The angle between the *x*-axis and RNA trimer dilution curve is $56^\circ \pm 2^\circ$ (Table 1, Fig. 5).

In summary, one pRNA building block, not the hexamer, is regarded as one functional unit. Since six monomeric pRNA is needed to build a hexamer, the stoichiometry for momomer pRNA is six (Fig. 4A). Since three pRNA dimers are needed to build a hexamer, the stoichiometry for pRNA dimer is three (Fig. 4B). Since two trimeric pRNA is needed to build a hexamer, the stoichiometry for pRNA trimer is two (Fig. 4C). As shown in Fig. 5, the slopes of log/log plot curves for trimeric, dimeric and monomeric pRNA descend with the stoichiometry, suggesting that slopes and stoichiometry are correlated.

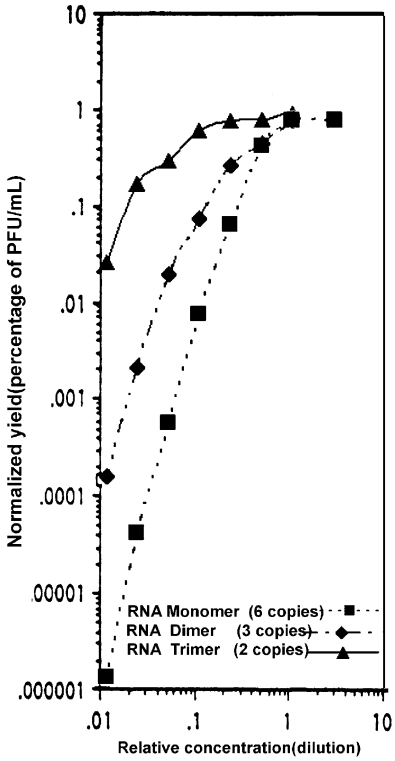

Fig. 5. Log/log plot of concentration vs. the yield of virus production for pRNA monomer, dimer, and trimer.

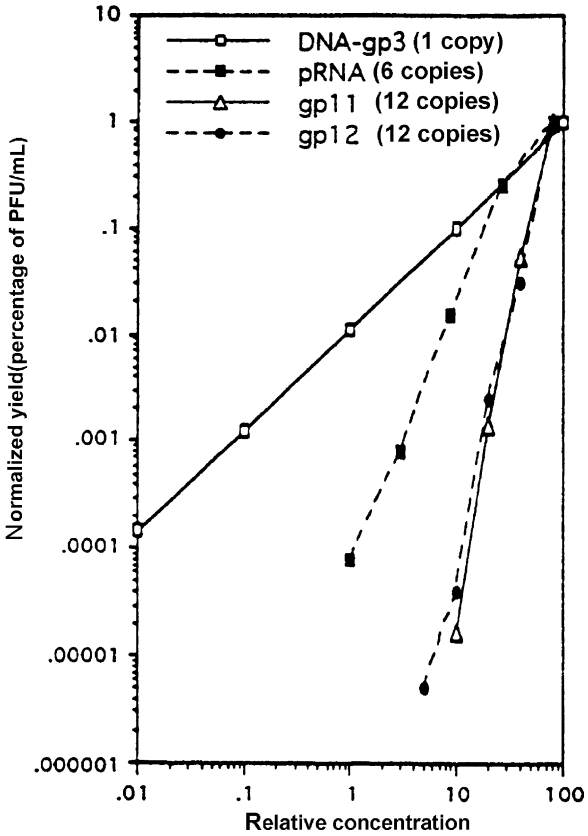

Fig. 6. Log/log plot of concentration vs. the yield of virus production for DNA–gp3, pRNA monomer, gp11 and gp12.

3.3.4. Slope descending for gp12/gp11 (stoichiometry of 12), monomer pRNA (stoichiometry of six) and DNA genome (stoichiometry of one)

The stoichiometry of the appendage gp12 and the lower collar gp11 has been determined to be 12 (Peterson et al., 2001). As noted earlier, the stoichiometry of monomer pRNA and genomic DNA–gp3 is six and one, respectively. As shown in Fig. 6, the slopes of log/log plot curves for gp12/gp11, monomer pRNA and genomic DNA–gp3 descends with the stoichiometry, again suggesting that slopes and stoichiometry are correlated. The angle between the *x*-axis and DNA–gp3, gp11 or gp12 dilution curve is 45°±4°, 79°±1°, and 80°±2°, respectively (Table 1, Fig. 6).

3.3.5. The slope of log/log plot curve for procapsid (stoichiometry of one) is smaller than the slope for the tail protein gp9 (stoichiometry of nine)

The stoichiometry of the tail protein gp9 has been determined to be nine (Peterson et al., 2001), and the stoichiometry of procapsid is one. The angle between the *x*-axis and prohead dilution curve is 47° ± 3°, while the angle between the *x*-axis and gp9 dilution curve is 77° ± 2° (Fig. 7, Table 1). The slopes of log/log plot curves for procapsid is smaller than the slope for gp9, suggesting that slopes and stoichiometry are correlated (Fig. 7).

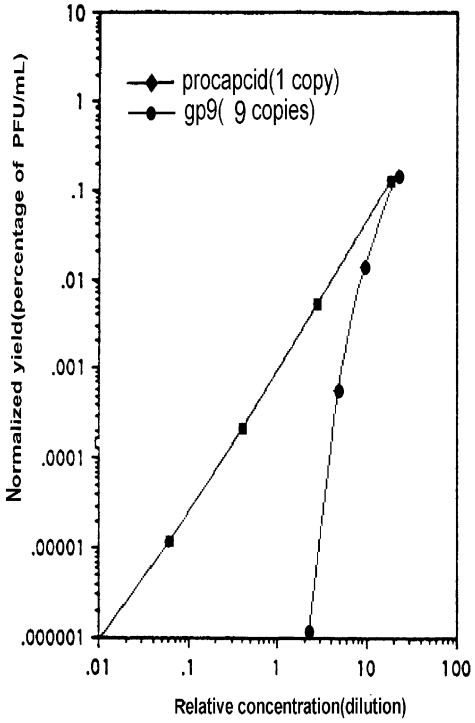

Fig. 7. Log/log plot of concentration vs. the yield of virus production for procapsid and gp9.

3.4. Deduction of equation for stoichiometry determination

The components, including procapsid, DNA–gp3, pRNA trimer, dimer and monomer as well as gp9, gp11 and gp12 that are needed for the in vitro phi29 assembly was assayed to determine their concentration dependent curves. Each component was assayed by serial dilution while keeping all other components optimal or excess. The log of the

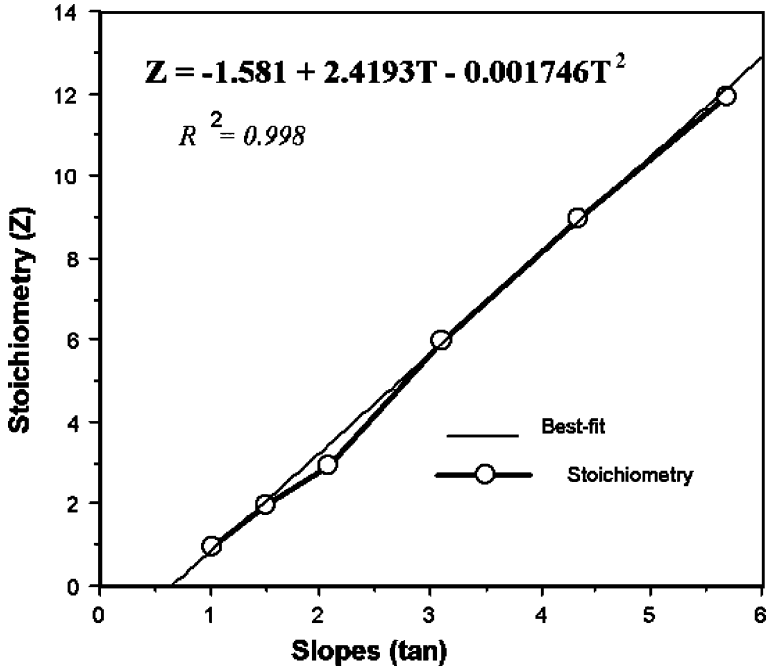

Fig. 8. Plotting of stoichiometry against slopes of dose-response log/log plot curves of components in phi29 assembly in vitro. The equations were derived from the best-fit curve with an R^2 of 0.998.

Table 2
Theoretical conversion table from stoichiometry to slopes

Stoichiometry	*Slopes (tan)*	Stoichiometry	*Slopes (tan)*	Stoichiometry	*Slopes (tan)*
1	*1*	**9**	*4.33*	**17**	*7.72*
2	*1.48*	**10**	*4.80*	**18**	*8.14*
3	*2.05*	**11**	*5.22*	**19**	*8.56*
4	*2.31*	**12**	*5.67*	**20**	*8.98*
5	*2.73*	**13**	*6.05*	**21**	*9.40*
6	*3.14*	**14**	*6.47*	**22**	*9.82*
7	*3.56*	**15**	*6.89*	**23**	*10.24*
8	*3.97*	**16**	7.31	**24**	*10.66*

Table 3
Stoichiometry prediction from slopes

Degrees	Slopes	Stoichio	Degrees	Slopes	Stoichio	Degrees	Slopes	Stoichio
45.0	1.0	0.8	80.5	6.0	12.9	84.8	11.0	24.8
47.7	1.1	1.1	80.7	6.1	13.1	84.9	11.1	25.1
50.2	1.2	1.3	80.8	6.2	13.4	84.9	11.2	25.3
52.4	1.3	1.6	81.0	6.3	13.6	84.9	11.3	25.5
54.5	1.4	1.8	81.1	6.4	13.8	85.0	11.4	25.8
56.3	1.5	2.0	81.3	6.5	14.1	85.0	11.5	26.0
58.0	1.6	2.3	81.4	6.6	14.3	85.1	11.6	26.2
59.5	1.7	2.5	81.5	6.7	14.5	85.1	11.7	26.5
60.9	1.8	2.8	81.6	6.8	14.8	85.2	11.8	26.7
62.2	1.9	3.0	81.8	6.9	15.0	85.2	11.9	27.0
63.4	2.0	3.3	81.9	7.0	15.3	85.2	12.0	27.2
64.5	2.1	3.5	82.0	7.1	15.5	85.3	12.1	27.4
65.6	2.2	3.7	82.1	7.2	15.7	85.3	12.2	27.7
66.5	2.3	4.0	82.2	7.3	16.0	85.4	12.3	27.9
67.4	2.4	4.2	82.3	7.4	16.2	85.4	12.4	28.1
68.2	2.5	4.5	82.4	7.5	16.5	85.4	12.5	28.4
69.0	2.6	4.7	82.5	7.6	16.7	85.5	12.6	28.6
69.7	2.7	4.9	82.6	7.7	16.9	85.5	12.7	28.9
70.3	2.8	5.2	82.7	7.8	17.2	85.5	12.8	29.1
71.0	2.9	5.4	82.8	7.9	17.4	85.6	12.9	29.3
71.6	3.0	5.7	82.9	8.0	17.7	85.6	13.0	29.6
72.1	3.1	5.9	83.0	8.1	17.9	85.6	13.1	29.8
72.6	3.2	6.1	83.0	8.2	18.1	85.7	13.2	30.0
73.1	3.3	6.4	83.1	8.3	18.4	85.7	13.3	30.3
73.6	3.4	6.6	83.2	8.4	18.6	85.7	13.4	30.5
74.1	3.5	6.9	83.3	8.5	18.9	85.8	13.5	30.8
74.5	3.6	7.1	83.4	8.6	19.1	85.8	13.6	31.0
74.9	3.7	7.3	83.4	8.7	19.3	85.8	13.7	31.2
75.3	3.8	7.6	83.5	8.8	19.6	85.9	13.8	31.5
75.6	3.9	7.8	83.6	8.9	19.8	85.9	13.9	31.7
76.0	4.0	8.1	83.7	9.0	20.1	85.9	14.0	31.9
76.3	4.1	8.3	83.7	9.1	20.3	85.9	14.1	32.2
76.6	4.2	8.5	83.8	9.2	20.5	86.0	14.2	32.4
76.9	4.3	8.8	83.9	9.3	20.8	86.0	14.3	32.7
77.2	4.4	9.0	83.9	9.4	21.0	86.0	14.4	32.9
77.5	4.5	9.3	84.0	9.5	21.2	86.1	14.5	33.1
77.7	4.6	9.5	84.1	9.6	21.5	86.1	14.6	33.4
78.0	4.7	9.8	84.1	9.7	21.7	86.1	14.7	33.6
78.2	4.8	10.0	84.2	9.8	22.0	86.1	14.8	33.8
78.5	4.9	10.2	84.2	9.9	22.2	86.2	14.9	34.1
78.7	5.0	10.5	84.3	10.0	22.4	86.2	15.0	34.3
78.9	5.1	10.7	84.3	10.1	22.7	86.2	15.1	34.6
79.1	5.2	11.0	84.4	10.2	22.9	86.2	15.2	34.8
79.3	5.3	11.2	84.5	10.3	23.2	86.3	15.3	35.0
79.5	5.4	11.4	84.5	10.4	23.4	86.3	15.4	35.3
79.7	5.5	11.7	84.6	10.5	23.6	86.3	15.5	35.5
79.9	5.6	11.9	84.6	10.6	23.9	86.3	15.6	35.7
80.0	5.7	12.2	84.7	10.7	24.1	86.4	15.7	36.0
80.2	5.8	12.4	84.7	10.8	24.3	86.4	15.8	36.2
80.4	5.9	12.6	84.8	10.9	24.6	86.4	15.9	36.4

concentration (*x*-axis, from low to high) was plotted versus the log of the yield (*y*-axis, PFU/ml). The unit length of the log scale of *x*-axis and *y*-axis were equal in the plot to determine the angle between the *x*-axis and the concentration depend curve (Figs. 5–7). The value of tangent (slope, tan) for the angle of the procapsid, DNA–gp3, pRNA trimer, dimer, and monomer, as well as gp9, gp11 and gp12 were obtained (Table 1). The slopes (tan) of all curves were plotted against their stoichiometry. A computer program Cricket Graph was used to find a best-fit curve and to deduce the formula for stoichiometry determination.

Four formulas were tested for their suitability in stoichiometry determination for the third step. These formulas include Polynomial ($Z = m + k_1T + k_2T^2 + \cdots$), Logarithmic [$Z = (m + k \times \log(T)$], Exponential ($Z = mn^{kT}$) and a simple equation ($Z = m + kT$), where Z is the stoichiometry, T is the slope that is equal to tan $\angle\alpha$ (α is the angle between the curve and the *x*-axis), and k and m are constants that were determined empirically. With the experimental data in Table 1, it was found that the polynomial with two orders is the best fit, as suggested by the R^2 value of 0.998 (Fig. 8). When the log of dose response curves or dilution factor is plotted against the log of the yield of the reaction, the stoichiometry Z can be determined with an equation, $Z = -1.58 + 2.4193T - 0.001746T^2$ [$T \in (0,1000)$, or $\angle\alpha \in (0^\circ, 89.9^\circ)$], where T is the slope of the curve, that is the tangent of $\angle\alpha$, which was defined as the angle between the curve and the *x*-axis. This equation was also examined for its feasibility in stoichiometry determination. It was found that the stoichiometry could be determined by these formulas with a high reliability (Tables 1 and 2). For example, the angle of the curve representing gp12 was determined to be 80° (Fig. 6), so $T = \tan\angle 80^\circ = 5.67$. From equation $Z = -1.58 + 2.4193T - 0.001746T^2$, if $T = 5.67$, $Z = 12.1$. The theoretical calculation of stoichiometry of gp12 should be 12. It agrees with the stoichiometry of gp12 that has been determined previously (Peterson et al., 2001; Tosi et al., 1975; Villanueva et al., 1981; Villanueva and Salas, 1981). Table 3 is the predicted parameters using the equation $Z = -1.58 + 2.4193T - 0.001746T^2$.

4. Discussion

Reusability of the component can interfere with and complicate the results when using this log/log slope assay method for stoichiometry determination. The principle for the determination of stoichiometry by this method is based on the related concentration of the components. If a component is reusable, the outcome of quantification will not be reliable in comparison with components that are non-reusable. If the component is reusable, the recycled molecules will add to the pool of molecules that are able to function in in vitro assembly. The concentration will appear higher than it actually is and thus the stoichiometry determined will be lower than the real number. Gp16, the DNA-packaging enzyme of phi29, is such a re-usable component. The determination of stoichiometry of gp16 proved to be difficult, that is why the stoichiometry quantification of gp16 is excluded from this report.

Acknowledgements

We would like to thank, Jane Kovach, Songchuan Guo and Sonia Soto for assistance in the preparation of the manuscript. This work was supported by NIH grant GM59944.

References

Anderson, D.L., Hickman, H.H., Reilly, B.E., 1966. Structure of *bacillus subtilis* bacteriophage phi29 and the length of phi29 deoxyribonucleic acid. J. Bacteriol. 91, 2081–2089.

Balzani, V., Credi, A., Venturi, M., 2002. The bottom-up approach to molecular-level devices and machines. Chemistry 8, 5524–5532.

Bancroft, J.B., Hills, G.J., Markham, R., 1967. A study of the self-assembly process in a small spherical virus. formation of organized structures from protein subunits in vitro. Virology 31, 354.

Bazinet, C., King, J., 1985. The DNA translocation vertex of dsDNA bacteriophages. Ann. Rev. Microbiol. 39, 109–129.

Becker, A., Marko, M., Gold, M., 1977. Early events in the in vitro packaging of bacteriophage DNA. Virology 78, 291–305.

Black, L.W., 1989. DNA packaging in dsDNA bacteriophages. Ann. Rev. Microbiol. 43, 267–292.

Carbone, A., Seeman, N.C., 2002. Circuits and programmable self-assembling DNA structures. Proc. Natl. Acad. Sci. U.S.A. 99, 12577–12582.

Chen, C., Guo, P., 1997a. Magnesium-induced conformational change of packaging RNA for procapsid recognition and binding during phage phi29 DNA encapsidation. J. Virol. 71, 495–500.

Chen, C., Guo, P., 1997b. Sequential action of six virus-encoded DNA-packaging RNAs during phage phi29 genomic DNA translocation. J. Virol. 71, 3864–3871.

Chen, C., Trottier, M., Guo, P., 1997. New approaches to stoichiometry determination and mechanism investigation on RNA involved in intermediate reactions. Nucleic Acids Symp. Ser. 36, 190–193.

Chen, C., Zhang, C., Guo, P., 1999. Sequence requirement for hand-in-hand interaction in formation of pRNA dimers and hexamers to gear phi29 DNA translocation motor. RNA 5, 805–818.

Chen, C., Sheng, S., Shao, Z., Guo, P., 2000. A dimer as a building block in assembling RNA. a hexamer that gears bacterial virus phi29 DNA-translocating machinery. J. Biol. Chem. 275 (23), 17510–17516.

Cohen, F.E., Abarbanel, R.A., Kuntz, I.D., Fletterick, R.J., 1986. Turn prediction in proteins using a pattern-matching approach. Biochemistry 25, 266–275.

D'Halluin, J.-C., Martin, G.R., Torpier, G., Boulanger, P.A., 1978. Adenovirus type 2 assembly analyzed by reversible crosslinking of labile intermediates. J. Virol. 26, 357–363.

Dujardin, E., Peet, C., Stubbs, G., Culver, J.N., Mann, S., 2003. Organization of metallic nanoparticles using tobacco mosaic virus templates. Nano Lett. 3 (3), 413–417.

Earnshaw, W.C., Casjens, S.R., 1980. DNA packaging by the double-stranded DNA bacteriophages. Cell 21, 319–331.

Edvardsson, B., Everitt, E., Joernvall, E., Prage, L., Philipson, L., 1976. Intermediates in adenovirus assembly. J. Virol. 19, 533–547.

Fraenkel-Conrat, H., Williams, R.C., 1955. Reconstitution of active tobacco mosaic virus from its inactive protein and nucleic acid components. Proc. Natl. Acad. Sci. U.S.A. 41, 690–698.

Garver, K., Guo, P., 1997. Boundary of pRNA functional domains and minimum pRNA sequence requirement for specific connector binding and DNA packaging of phage phi29. RNA 3, 1068–1079.

Garver, K., Guo, P., 2000. Mapping the inter-RNA interaction of phage phi29 by site-specific photoaffinity crosslinking. J. Biol. Chem. 275 (4), 2817–2824.

Guasch, A., Pous, J., Ibarra, B., Gomis-Ruth, F.X., Valpuesta, J.M., Sousa, N., Carrascosa, J.L., Coll, M., 2002. Detailed architecture of a DNA translocating machine: the high-resolution structure of the bacteriophage phi29 connector particle. J. Mol. Biol. 315, 663–676.

Guo, P., 1994. Introduction: principles, perspectives, and potential applications in viral assembly. Semin. Virol. (Editor's Introduction) 5 (1), 1–3.

Guo, P., 2002a. Methods for structural and functional analysis of an RNA hexamer of bacterial virus phi29 DNA packaging motor. Acta Biochim. Biophys. Sinca 34, 533–543.

Guo, P., 2002b. Structure and function of phi29 hexameric RNA that drive viral DNA packaging motor: review. Prog. Nucleic. Acid Res. Mol. Biol. 72, 415–472.

Guo, P., Grimes, S., Anderson, D., 1986. A defined system for in vitro packaging of DNA–gp3 of the *bacillus subtilis* bacteriophage phi29. Proc. Natl. Acad. Sci. U.S.A. 83, 3505–3509.

Guo, P., Erickson, S., Anderson, D., 1987. A small viral RNA is required for in vitro packaging of bacteriophage phi29 DNA. Science 236, 690–694.

Guo, P., Erickson, S., Xu, W., Olson, N., Baker, T.S., Anderson, D., 1991. Regulation of the phage phi29 prohead shape and size by the portal vertex. Virology 183, 366–373.

Guo, P., Zhang, C., Chen, C., Trottier, M., Garver, K., 1998. Inter-RNA interaction of phage phi29 pRNA to form a hexameric complex for viral DNA transportation. Mol. Cell 2, 149–155.

Hendrix, R.W., 1998. Bacteriophage DNA packaging: RNA gears in a DNA transport machine (minireview). Cell 94, 147–150.

Hill, A.V., 1910. The combinations of haemoglobin with oxygen and with carbon monoxide. J. Physiol. 40, iv–vii.

Hoeprich, S., Guo, P., 2002. Computer modeling of three-dimensional structure of DNA-packaging RNA(pRNA) monomer, dimer, and hexamer of Phi29 DNA packaging motor. J. Biol. Chem. 277 (23), 20794–20803.

Hohn, B., 1975. DNA as substrate for packaging into bacteriophage lambda, in vitro. J. Mol. Biol. 98, 93–106.

Hsiao, C.L., Black, L.W., 1977. DNA packaging and the pathway of bacteriophage T4 head assembly. Proc. Natl. Acad. Sci. U.S.A. 74, 3652–3656.

Hyman, P., Valluzzi, R., Goldberg, E., 2002. Design of protein struts for self-assembling nanoconstructs. Proc. Natl. Acad. Sci. U.S.A. 99, 8488–8493.

Ibarra, B., Caston, J.R., Llorca, O., Valle, M., Valpuesta, J.M., Carrascosa, J.L., 2000. Topology of the components of the DNA packaging machinery in the phage phi29 prohead. J. Mol. Biol. 298, 807–815.

Israel, J.V., Anderson, T.H., Levine, M., 1967. In vitro morphogenesis of phage p22 from heads and base-plate parts. Proc. Natl. Acad. Sci. U.S.A. 57, 284–291.

Kaiser, D., Masuda, T., 1973. In vitro assembly of bacteriophage lambda heads. Proc. Natl. Acad. Sci. U.S.A. 70, 260–264.

Kaiser, A.D., Syvanen, M., Masuda, T., 1975. DNA packaging steps in bacteriophage lambda head assembly. J. Mol. Biol. 91, 175–186.

Kerr, C., Sadowski, P.D., 1974. Packaging and maturation of DNA of bacteriophage T7 in vitro. Proc. Natl. Acad. Sci. U.S.A. 71, 3545–3549.

King, J., Casjens, S., 1974. Catalytic head assembly protein in virus morphogenesis. Nature 251, 112–119.

Lee, C.S., Guo, P., 1994. A highly sensitive system for the in vitro assembly of bacteriophage phi29 of *bacillus subtilis*. Virology 202, 1039–1042.

Lee, C.S., Guo, P., 1995a. In vitro assembly of infectious virions of dsDNA phage phi29 from cloned gene products and synthetic nucleic acids. J. Virol. 69, 5018–5023.

Lee, C.S., Guo, P., 1995b. Sequential interactions of structural proteins in phage phi29 procapsid assembly. J. Virol. 69, 5024–5032.

Lee, S.W., Mao, C., Flynn, C.E., Belcher, A.M., 2002. Ordering of quantum dots using genetically engineered viruses. Science 296, 892–895.

Leibowitz, J., Horwitz, M.S., 1975. Synthesis and assembly of adenovirus polypeptieds. III. Reversible inhibition of hexon assembly at 42C. Virology 66, 10–24.

Miyazaki, J., Fugisawa, H., Minagawa, T., 1978. Biological activity of purified bacteriophage T3 prohead and prohead-like stuctures as precusors for in vitro head assembly. Virology 91, 283–290.

Moll, D., Huber, C., Schlegel, B., Pum, D., Sleytr, U.B., Sara, M., 2002. S-layer-streptavidin fusion proteins as template for nanopatterned molecular arrays. Proc. Natl. Acad. Sci. U.S.A. 99, 14646–14651.

Monod, J., Wyman, J., Changeux, J., 1965. On the nature of allosteric transitions: a plausible model. J. Mol. Biol. 12, 88–118.

Morais, M.C., Tao, Y., Olsen, N.H., Grimes, S., Jardine, P.J., Anderson, D., Baker, T.S., Rossmann, M.G., 2001. Cryoelectron-Microscopy Image Reconstruction of Symmetry Mismatches in Bacteriophage phi29. J. Struct. Biol. 135, 38–46.

Murialdo, H., Becker, A., 1977. Assembly of biologically active proheads of bacteriophage lambda in vitro. Proc. Natl. Acad. Sci. U.S.A. 74, 906–910.

Niemeyer, C.M., 2002. The developments of semisynthetic DNA-protein conjugates. Trends Biotechnol. 20, 395–401.

Peterson, C., Simon, M., Hodges, J., Mertens, P., Higgins, L., Egelman, E., Anderson, D., 2001. Composition and mass of the bacteriophage phi29 prohead and virion. J. Struct. Biol. 135, 18–25.

Pruss, G.J., Wang, J.C., Calendar, R., 1975. In vitro packaging of covalently closed monomers of bacteriophage DNA. J. Mol. Biol. 98, 465–478.

Seeman, N.C., Belcher, A.M., 2002. Emulating biology: building nanostructures from the bottom up. Proc. Natl. Acad. Sci. U.S.A. 99 (2), 6451–6455.

Shu, D., Guo, P., 2003. A viral RNA that binds ATP and contains an motif similar to an ATP-binding aptamer from SELEX. J. Biol. Chem. 278 (9), 7119–7125.

Simpson, A.A., Tao, Y., Leiman, P.G., Badasso, M.O., He, Y., Jardine, P.J., Olson, N.H., Morais, M.C., Grimes, S., Anderson, D.L., Baker, T.S., Rossmann, M.G., 2000. Structure of the bacteriophage phi29 DNA packaging motor. Nature 408, 745–750.

Skehel, J., Joklik, W., 1969. Studies on the in vitro transcription of reovirus RNA catalyzed by reovirus cores. Virology 39, 822–831.

Thomas, D., Prevelige, P., 1991. A pilot protein participates in the initiation of P22 procapsid assembly. Virology 182, 637–681.

Tosi, M.E., Reilly, B.E., Anderson, D.L., 1975. Morphogenesis of bacteriophage phi29 of *bacillus subtilis*: cleavage and assembly of the neck appendage protein. J. Virol. 16, 1282–1295.

Trottier, M., Guo, P., 1997. Approaches to determine stoichiometry of viral assembly components. J. Virol. 71, 487–494.

Trottier, M., Mat-Arip, Y., Zhang, C., Chen, C., Sheng, S., Shao, Z., Guo, P., 2000. Probing the structure of monomers and dimers of the bacterial virus phi29 hexamer RNA complex by chemical modification. RNA 6, 1257–1266.

Villanueva, N., Salas, M., 1981. Adsorption of bacteriophage phi29 to *bacillus subtilis* through the neck appendage of the viral particle. J.Virol. 38 (1), 15–19.

Villanueva, N., Lazaro, J.M., Salas, M., 1981. Purification, properties and assembly of the neck-appendage protein of the *bacillus subtilis* phage phi29. Eur. J. Biochem. 117, 499–505.

Waterman, M.S., Gordon, L., Arratia, R., 1987. Phase transitions in sequence matches and nucleic acid structure. Proc. Natl. Acad. Sci. U.S.A. 84, 1239–1243.

Weiss, J.N., 1997. The Hill equation revisited: uses and misuses. FASEB J. 11, 835–841.

White, J.H., Cozzarelli, N.R., Bauer, W.R., 1988. Helical repeat and linking number of surface-wrapped DNA. Science 241, 323–327.

Wilhelm, J., Ginsberg, H.S., 1972. Synthesis in vitro of type 5 adenovirus capsid proteins. J. Virol. 9, 973–980.

Zhang, C.L., Lee, C.-S., Guo, P., 1994. The proximate 5′ and 3′ ends of the 120-base viral RNA (pRNA) are crucial for the packaging of bacteriophage phi29 DNA. Virology 201, 77–85.

Zhang, F., Lemieux, S., Wu, X., St.-Arnaud, S., McMurray, C.T., Major, F., Anderson, D., 1998. Function of hexameric RNA in packaging of bacteriophage phi29 DNA in vitro. Mol. Cell 2, 141–147.